Downloaded from http://jgs.lyellcollection.org/ at Orta Dogu Teknik Universitesi on April 5, 2016
Journal of the Geological Society, London, Vol. **164**, 2007, pp. 393–404. Printed in Great Britain.

Thermo-chronology of the Barlet metamorphic basement unit: evidence for a Stephanian thermal event linked to Sb mineralization in the Haut Allier, France

VINCENT J. VAN HINSBERG[1,4], ENNO ZINNGREBE[2], HANNO DE WIJS[3] & SIMON P. VRIEND[3]

[1]*Department of Earth Sciences, University of Bristol, Wills Memorial Building, Queens Road, Bristol BS8 1RJ, UK (e-mail: V.J.vanHinsberg@gmx.net)*

[2]*Ceramics Research Centre, Corus RD&T, IJmuiden, Netherlands*

[3]*Faculteit Aardwetenschappen, Universiteit Utrecht, Budapestlaan 4, 3584 CD, Utrecht, Netherlands*

[4]*Present address: Department of Earth & Planetary Sciences, McGill University, 3450 University Street, Montreal, Quebec, H3A 2A7, Canada*

Abstract: A thermo-chronological analysis of the Barlet basement unit (French Massif Central) reveals a four-stage history. Peak metamorphism (650 °C and 7 kbar) was followed by retrograde growth of albite blasts and development of the main foliation at 600 °C, and chloritization of the ferromagnesian minerals. The third stage is a marked reversal of cooling, with recrossing of the biotite isograd and local reappearance of garnet at 450 °C. This thermal event, inferred to result from hot fluid infiltration, is also recognized in the adjacent basin of Langeac, where it gives rise to anomalous coal grades (recording 200 °C at 1 km). A Stephanian age for this event correlates with a regional thermal event recognized throughout the Variscan, where it has been linked to delamination of the continental crust. This work represents the first instance in the Massif Central that recognizes this event in the shallow basement itself. Final cooling is accompanied by extensive fluid-induced sericitization, starting immediately after the peak of the thermal event and continuing to temperatures inferred for Sb–As ore deposition. This continuum leads us to conclude that reheating-related silicate reactions and ore deposition are caused by the same fluid and related to the wider regional Variscan thermal event.

The thermo-chronological history of the Variscan orogeny has received considerable attention (e.g. Scaillet *et al*. 1996; Bouchot *et al*. 1997; Faure *et al*. 2002). This is because it is linked to both the nature of the change from orogenic compression to continental collapse and the metallogeny of widespread late Variscan hydrothermal mineralization. In the Massif Central the transition from compression to extension is rapid and marked by the development of numerous basins with Stephanian to Permian volcano-sedimentary infill, culminating in a 'Basin and Range' morphology in the Permian (Ménard & Molnar 1988; Malavieille *et al*. 1990). This change-over to extensional tectonics is accompanied by a distinct thermal event, which is time-offset from the main period of late orogenic granite magmatism (Viséan to Namurian; Ploquin & Stussi 1994; Marignac & Cuney 1999).

Expressions of this thermal event are varied. Forward modelling of the thermo-chronological evolution of mid-crustal laccoliths in the St-Sylvestre area using $^{40}Ar/^{39}Ar$ muscovite ages (Scaillet *et al*. 1996) has shown that their cooling and exhumation history cannot be explained without a prolonged heat-flow increase following their emplacement at 324 ± 4 Ma. The preferred model of Scaillet *et al*. invokes an episodically increased heat flow during much of the Westphalian, ending at about 305 Ma. Similarly, anomalously high heat flow or thermal perturbations are inferred from studies of coal-bearing Stephano-Permian basins throughout the Massif Central. Golitsyn *et al*. (1997) found evidence for rapid coalification associated with fault-controlled fluid-convective heating, whereas Copard *et al*. (2000) inferred elevated heat-flow values of up to 180 mW m^{-2} from coal maturity in various Stephanian basins. Recent reinvestigations of Au–As hydrothermal vein deposits led Bouchot *et al*. (1997) to pinpoint mineralized zones within the Massif Central identified as palaeo-hydrothermal fields active within the Stephanian. The formation of the anatectic Velay dome under high-temperature–low-pressure (HT–LP) conditions has also been associated with this event (Marignac & Cuney 1999). The nature and causes of this late thermal event are still unclear, but have been linked to lithospheric delamination below the thickened continental crust, which allowed upward transmittance of asthenospheric heat (Malavieille *et al*. 1990; Marignac & Cuney 1999; Ledru *et al*. 2001).

Whereas evidence for a post-orogenic thermal event is widespread in the Massif Central, the volume of observations is still scanty. Most notably, this event has not been reported in the shallow metamorphic basement. Without knowing the impact of this thermal event on the shallow basement, its evolution and upper crustal significance cannot be properly assessed. Here, we have undertaken a detailed thermo-chronological study of the metamorphic basement of the Barlet area in the Haut Allier, one of the classical, well-investigated areas of the Massif Central nappe pile. The main advantage of selecting this area lies in the direct superimposition of several of the phenomena that are linked to a post-orogenic thermal event. The study area lies south of the village of Langeac, comprising the southern end of the Haut Allier Nappe complex, and including the Stephanian coal-bearing Langeac basin (Fig. 1). It is centred around the former mining district of Barlet, which exploited Sb–As hydrothermal vein deposits and extensive fluorite–barite deposits of the Langeac Fluorite Belt (Bril *et al*. 1994). The nature of the Barlet area rocks and their apparent incompatibility with the published lithology for the area requires us to first introduce the Barlet unit and its regional context, before going into its thermal history.

Downloaded from http://jgs.lyellcollection.org/ at Orta Dogu Teknik Universitesi on April 5, 2016

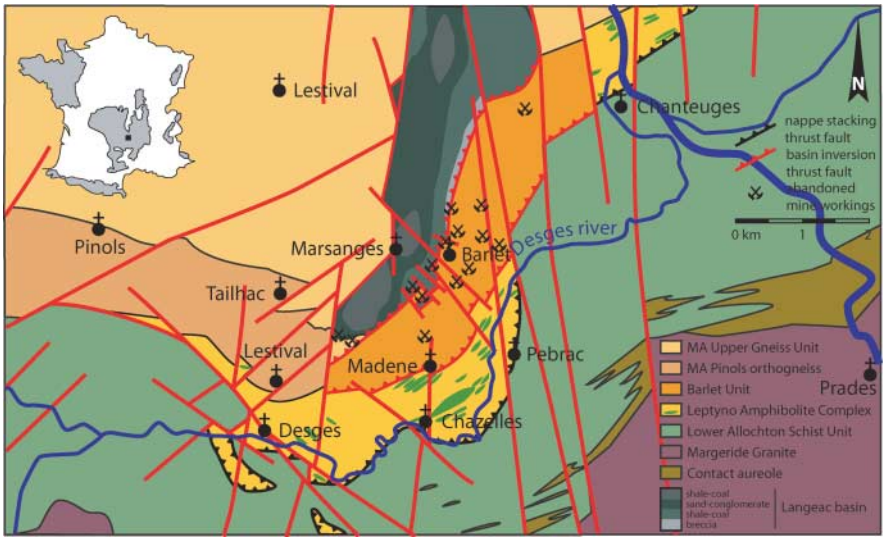


Fig. 1. Overview map of the study area in the French Massif Central (see inset). The Barlet unit is present as a thrust-sheet on top of, and in part completely overriding, the Leptyno-Amphibolite Complex. It is bordered in the east by Lower Allochthon schists and in the north by the sedimentary basin of Langeac. Outcrops of Margeride granite with associated contact aureole are present in the SE. Map modified after Marchand *et al*. (1989).

Regional geology

Variscan basement

The basement of the study area (Fig. 1) represents a cross-section through the Haut Allier nappe pile, consisting of a 'Middle Allochthon' (an anatectic thrust sheet) that has overridden a 'Lower Allochthon' along a strongly mylonitized thrust zone.

The Middle Allochthon is separated (Burg *et al*. 1984; Ledru *et al*. 1989, 1994; Matte 1991) into a main body of anatectic gneisses (the upper gneiss unit) resting on top of a heterogeneous 'Leptyno-Amphibolite Complex'. The latter accommodates most of the overthrust shear and is characterized by the presence of metabasic boudins in a mylonitic matrix. The upper gneiss unit experienced peak conditions up to granulite facies (14 kbar, 800 °C; Santallier *et al*. 1994), followed by extensive decompression melting during nappe stacking. These melts now form discordant leucogranitic bodies. The metamorphic conditions for the Leptyno-Amphibolite Complex rocks are varied, reflecting the varied lithologies present in this unit, with the metabasic boudins preserving relicts of an early high-pressure history up to eclogite facies (see Forestier 1961). However, the dominant metamorphic conditions preserved in the Leptyno-Amphibolite Complex, middle amphibolite facies, are related to thrusting and development of mylonitic textures.

The 'orthogneiss of Pinols' (see Fig. 1) is a distinct, lens-shaped intercalation of granitoid gneisses on the southern border of the upper gneiss unit (Marchand *et al*. 1989). This body has been interpreted as a pre-metamorphic granite. It is characterized by a lineation-dominated fabric and is nearly devoid of ferromagnesian phases. It has been subjected to the same high-grade conditions as the bulk of the upper gneiss unit, although original magmatic textures are locally preserved.

The Lower Allochthon is a mainly pelitic unit that is exposed in the study area in a tectonic window along the Desges river valley (Fig. 1). The unit consists of pelitic to psammitic schists with a general assemblage of garnet–staurolite–biotite ± relicts of sillimanite. The peak metamorphic conditions are confined to middle amphibolite-facies conditions (650–700 °C, 8 kbar, Santallier *et al*. 1994), some 100 °C lower than anatectic conditions in the upper gneiss unit. A mappable zone within this succession yields relicts of kyanite. Retrogression with production of muscovite at the expense of K-feldspar and sillimanite is extensive, commonly completely overprinting older fabrics.

The metamorphic nappe sequence is intruded by the Margeride Granite, which crops out south of the Desges valley. This voluminous (3000 km^2, Couturié *et al*. 1979) porphyritic peraluminous granite massif (the AKG type of Ploquin & Stussi 1994) is characterized by megacrysts of K-feldspar. Estimates of its intrusion age range from 334 ± 7 Ma (U–Pb on zircon, Respaut 1984) to 323 ± 12 Ma (Rb–Sr whole-rock isochron age, Couturié *et al*. 1979). It is cut by younger leucogranite dykes (Westphalian, Couturié & Vachette 1980; Lafon & Respaut 1988; Marchand *et al*. 1989). The contact aureole of the Margeride Granite is not pronounced in the Desges valley and is characterized by a distinct lack of mineralogical changes in the Lower Allochthon host schists. It appears confined to textural changes (strain relaxation of the quartz fabrics). However, andalusite present in quartz veins in the vicinity of the Margeride Granite has been attributed to associated fluid circulation (Marchand *et al*. 1989).

Langeac Basin

The transition from compression to extension in the Neo-Variscan resulted in the formation of intramontane basins throughout the Massif Central (Faure 1995; Marignac & Cuney 1999). These basins, active from the Westphalian to the Permian, are interpreted as half-grabens and pull-apart basins along crustal-scale transcurrent fault systems (Faure 1995). The basin of Langeac in the study area (Fig. 1) is such a pull-apart basin. It is stratigraphically equivalent to the basins of St Etienne, Messeix–Singles, Graissesac, Brassac and Blanzy–Montceau (Amiot 1881; Robert *et al*. 1988; Marchand *et al*. 1989; Robert 1989; Courel & Liu 1991; Marignac & Cuney 1999), but has been little investigated because of its small size (2 km × 6 km).

The sedimentary infill of the basin has been divided into four units (Fig. 1), consisting of conglomerates and coarse sandstones, interrupted by two coal-bearing shaly sequences of lacustrine affinity (Amiot 1881; Marchand *et al*. 1989; unpublished mining reports; and our own work). The base of the succession consists of a locally derived breccia, grading into the country rock. The total thickness of sediments exposed on the surface and in coal mines is less than 1 km. The strata are characterized by rapid lateral facies changes and are interpreted as alluvial fan deposits. Conglomerate pebbles are dominated by weathered high-grade gneisses similar to those of the upper gneiss unit and by frequent hydrothermal quartz clasts. They specifically do not contain

Downloaded from http://jgs.lyellcollection.org/ at Orta Dogu Teknik Universitesi on April 5, 2016

amphibolites that might have been derived from the Leptyno-Amphibolite Complex unit. The shaly sequences are finely layered and grade from clay-rich to quartzose, with interbedded seams of coal. Three main coal seams were mined in the basin at the end of the 19th century, and their tailings provide access to material from deeper levels of the basin. The coals of the upper shaly sequence are high- to medium-volatile bituminous coals with a volatile content (V^{daf}) between 24.5 and 25.6% and a vitrinite reflectance of 1.3% (Amiot 1881; unpublished mining reports; and our own work). The coals in the lower sequence are of higher grade, with a V^{daf} of 19.3 and 14.1% and a vitrinite reflectance of 1.5 and 1.8% for two mining areas, respectively. Based on the fossil content of the coals, the age of these sediments has been determined to span the Stephanian A and B (Marchand *et al*. 1989).

The Langeac basin was subsequently deformed with fold axes aligned approximately parallel to the current basin margins. In places of strong lithological contrast, individual clastic beds are dismembered and have behaved as boudins in a sheared shale matrix. This period of basin inversion must be younger than Stephanian B in age, but the presence of resedimented coaly clasts indicates that tectonic activity started before sedimentation ceased. The coal grade follows the folding (Amiot 1881; unpublished mining reports), indicating that coalification of organic matter must predate folding and basin inversion. This has also been reported for the Messeix–Singles and Lorraine coal-bearing basins (Robert *et al*. 1988; Courel & Liu 1991).

Based on our mapping, we interpret the basin margins as overthrusts, reactivating the strike-slip faults along which the basin was originally opened. Direct proof of this is available for the southeastern margin fault, where erosion and mine collapse have exposed a 'klippe' of basin clastic rocks resting on metamorphic basement. Here, a thrust plane with coal and shale material along the fault gouge is well exposed. We extend this thrust interpretation to the western basin margin, which is known from mine reports to be subvertical at depth, but where gneiss is known to rest on sediments near Langeac (Amiot 1881; Marchand *et al*. 1989). Both the western and the eastern marginal thrusts are segmented by younger cross-cutting, subvertical faults with a strike varying from NW–SE to north–south. These faults also displace interior folds in the basin and can be correlated with faults identified in the Desges river valley metamorphic basement and offsetting the Margeride granite (Marchand *et al*. 1989).

Barlet unit

The main area of investigation is the segment of metamorphic basement separating the Langeac basin from the Leptyno-Amphibolite Complex and Lower Allochthon exposed in the Desges valley (Fig. 1). This segment forms a crest-line of hills running NE–SW approximately from Chanteuges on the river Allier to Lestival in the south, where it links up with the orthogneiss of Pinols. Previous mapping (Marchand *et al*. 1989) has included the bulk of this basement complex in the Leptyno-Amphibolite Complex of the Desges window. However, the lithology of the area does not support this assignment. The Desges Leptyno-Amphibolites are characterized by a high and characteristic content of mafic sheared boudins (Fig. 1). Neither mafic boudins nor the characteristic mylonitic leptynites of the Leptyno-Amphibolite Complex occur at Barlet. Also, although this complex is well exposed as a result of mining activity, there is a lack of massive banded or migmatized gneisses similar to those west of the Langeac Basin, which precludes its assignment to the upper gneiss unit. Because of these lithological contrasts, we have treated this area for the purposes of this study as a separate unit, named here the Barlet unit.

The Barlet unit, as defined here, consists of a tectonic mélange of quartzo-feldspathic gneisses, occurring as lens-shaped bodies of variable orientation and size (from hundreds of metres to decimetre scale) in a matrix of more or less homogeneous staurolite–garnet micaschists. The gneisses are characterized by a dominant linear fabric and scarcity of ferromagnesian phases, and thus resemble the orthogneiss of Pinols. The schist matrix, in turn, closely resembles the micaschists of the Lower Allochthon Desges exposures. Whereas this mélange character is similar to that of the Leptyno-Amphibolite Complex, both the nature of the boudins and the nature of the matrix are strongly different. A detailed map covering the best exposures of this tectonic mélange around the hamlet of Barlet is available online at http://www.geolsoc.org.uk/SUP18260. A hard copy can be obtained from the Society Library.

The unique character of the Barlet unit in contrast to the surrounding Lower Allochthon and Middle Allochthon units is also borne out by its numerous hydrothermal ore deposits. Undeformed mineralized veins extend into the Langeac basin, indicating that ore deposition postdates basin inversion. Two main types of mineralization are present: older vein deposits dominated by Sb–As sulphides, and younger fluorite deposits. Both types link up with regional ore provinces, with the Barlet unit constituting the eastern margin of the Brioude–Massiac Sb province (Périchaud 1980; Bril 1983), as well as being part of the Langeac–Lafayette Fluorite Belt (Derré 1972; Bril 1983). It is the only area where both are superimposed. An interesting correlation is also present between host lithology and Sb–As mineralization within the Barlet unit itself. Our mapping results show that the Sb–As veins are mineralized only where they cross the gneiss lenses, being barren along their extension into the schists (van Hinsberg *et al*. 2003).

Methods

Following detailed mapping, representative samples of each lithology were studied petrographically and mineral and whole-rock geochemistry analyses undertaken. Samples for whole-rock geochemistry by X-ray fluorescence (XRF) were crushed in a WC jaw-crusher and subsequently ground in an agate mill. An aliquot of 5 g of this powdered material was fired at 900 °C for 6 h in a porcelain cup to determine loss on ignition. A glass bead, containing 0.5 g of fired material, was prepared by fusing with 4.5 g of lithium borate flux at 1200 °C in an automated furnace. Reproducibility of the analyses was assessed by duplicates and is better than 1.5% relative for all major elements. Mineral analyses have been performed by wavelength-dispersive spectrometry (WDS) electron microprobe analysis and results are available online (see above). A hard copy can be obtained from the Society Library. Analyses labelled 'u' were carried out at Utrecht University on a Jeol JXA 8600 Pioneer probe, using a 10 μm spot size, 15 kV acceleration voltage and a beam current of 10 nA. A ZAF correction was applied to correct for matrix effects. Analyses labelled 'h' were carried out at the Geochemisches Institut of the Georg August University, Göttingen, Germany, on a Jeol JXA 8900 RL microprobe, using a spot size of 5 μm, 15 kV acceleration voltage and 15 nA beam current. A Phi-Rho-Z correction was applied to the data and corrections were made for spectral overlap of Fe on F, Ti on Ba, and Ba on Ti. Concentrations were standardized to: wollastonite (Si, Ca), corundum (Al), albite (Na), orthoclase (K), hematite (Fe), periclase (Mg), rutile (Ti), rhodonite (Mn), barite (Ba), topaz (F) and NaCl (Cl). Counting times were 30 s on peak for Mn, Ba, F and Cl, and 16 s for all other elements. The 1σ count statistical error on the analyses varies depending on the mineral, but was below 2.5% relative for the major elements and below 12% for the minor (<1 wt% absolute) elements. To

Downloaded from http://jgs.lyellcollection.org/ at Orta Dogu Teknik Universitesi on April 5, 2016

avoid underestimation of the Na content as a result of Na loss under the electron beam, Na was invariably analysed in the first spectrometer run.

Petrography and mineral chemistry of the Barlet unit

Gneiss lenses

The gneisses of the Barlet unit have a peak metamorphic assemblage of K-feldspar, plagioclase, biotite, quartz, ilmenite, apatite and zircon ± muscovite (Table 1). Sillimanite has not been observed. Although the mineralogy is constant between the lenses, mineral modes vary, as do textures. All the lenses have a well-developed foliation and mineral banding, as well as a strong linear fabric. In a number of lenses, especially where the mica content is low, the lineation becomes dominant, forming a rock composed of parallel quartzo-feldspathic rods. Two of the lenses contain centimetre-sized augen, consisting of clusters of K-feldspar, plagioclase and quartz, although K-feldspar is always dominant. The feldspars in these augen are patchily intergrown and preserve relicts of an equant, unfoliated inclusion assemblage (plagioclase, mica, quartz), suggesting a magmatic protolith for these rocks (Fig. 2a). Similar textures, although commonly not as well displayed, can be found in most of the other gneiss lenses as well.

Plagioclase compositions are close to the pure albite end-member (X_{An} <0.14) and some late-stage growth of plagioclase is evident from the presence of (mainly quartz) inclusions tracing an old foliation at the rim of the grains. The K-feldspar grains show perthitic exsolution of lamellae of Ab_{99} in an Or_{91} host. These lamellae make up about 20% of the total feldspar volume, giving an overall pre-exsolution composition of Or_{73}. These features are remarkably similar to those observed in parts of the orthogneiss of Pinols.

Schists

The schist matrix is lithologically homogeneous throughout the study area with a peak assemblage of garnet, staurolite, sillimanite, plagioclase, biotite, muscovite, ilmenite, graphite and quartz, with tourmaline as the main accessory (Table 1). The relative proportions of these minerals show some variation, especially in the amount of tourmaline present, and in the mica–quartz proportions. The schists have a well-developed foliation and crenulation that folds around the gneiss lenses. The dominant foliation in the schists is defined by muscovite and ilmenite, and wraps around the garnet and staurolite grains. However, this foliation overgrows an older foliation that is preserved by biotite, muscovite and sillimanite, as well as by inclusions of ilmenite, micas and quartz in mainly staurolite grains. The intimate intergrowth relations between these inclusions and their hosts suggests that this older foliation corresponds to peak metamorphic conditions. We will refer to these foliations as S_1 and S_3, with the crenulation being S_2 (Fig. 3), following Burg *et al*. (1984) and Ledru *et al*. (1994). However, there is evidence for a still older foliation preserved by ilmenite and quartz inclusions in the cores of tourmaline and garnet.

The micas preserve a multi-stage history (Table 1), starting with a peak metamorphic assemblage of biotite and muscovite (m_1, b_1). Biotite in this peak assemblage is intergrown with fibrolitic sillimanite and thin flakes of graphite. The development of crenulation results in folding and kinking of these mica bands, with a new generation of mainly muscovite growing in the kink bands (m_2, b_2). This is followed by muscovite overgrowing the older, folded and kinked mica generations (m_3). Overgrowth of

Table 1. *Overview of the stages recognized in Barlet unit schists and gneisses, and their stable mineral assemblages*

Stage		Details	Schist											Gneiss								
			garnet	staur	sil	mu	bio	chl	plag	qtz	graph	ilm	tour	K-feld	plag	mu	bio	chl	qtz	ilm	tour	stibnite
Prograde	a	gt & tour cores, ilm foliation, plag & K-feld intergrowth	+	–	–	+	+	–	–	+	–	+	+	+	+	+	+	–	+	+	+	–
Peak	b	Folded and kinked mu–bio foliation (S_1)	+	+	+	**+**	+	–	+	+	+	+	+	+	+	+	+	–	+	+	+	–
Retrograde	c 1	Albite blastesis, mu overgrowths	+	+	+	**+**	+	–	**+**	+	+	**+**	+	+	+	**+**	+	–	+	**+**	+	–
	2	Main mu–ilm foliation (S_3)	+	+	–	**+**	+	–	+	+	+	+	+	+	+	+	+	–	+	+	+	–
	3	Ferromagnesian phases to chlorite	–	–	–	+	–	+	+	+	–	+	+	+	+	+	–	–	+	+	+	–
Thermal event	d	New generation garnet + biotite	**+**	–	–	+	**+**	–	+	+	–	+	+	+	+	+	±	–	–	+	+	±
Final cooling	e 1	plag to sericite	–	–	–	**+**	–	–	–	+	–	–	+	–	±	+	–	–	+	+	+	–
	2	K-feld and mu to sericite; bio, gt and staur remnants to chl	–	–	–	–	–	+			–	–	+	–	–	–	–	**+**	+	–	+	

Symbols in bold denote a new generation of the mineral.

Downloaded from http://jgs.lyellcollection.org/ at Orta Dogu Teknik Universitesi on April 5, 2016

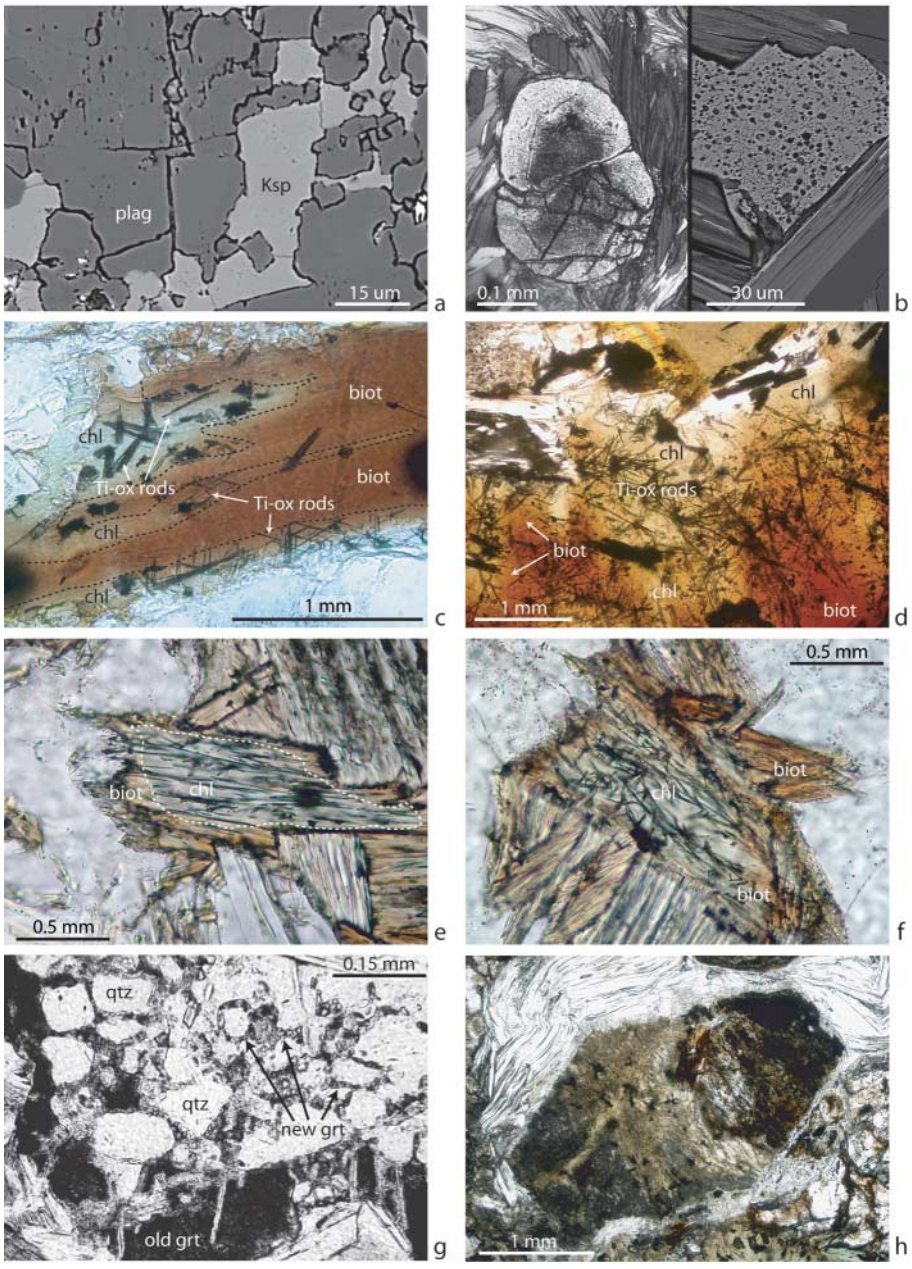


Fig. 2. (**a**) BSE image of undeformed magmatic intergrowth of K-feldspar and plagioclase preserved in an auge in one of the gneiss lenses. (**b**) Pits in a peak metamorphic garnet as seen in optical microscopy (left) and BSE imaging (right). Pits have negative garnet crystallography, and replace graphite inclusions. (**c**, **d**) Retrograde replacement of biotite by chlorite with development of rutile needles. The fresh, core section of biotite is devoid of rutile. (**e**, **f**) Replacement of chlorite by biotite with preservation of rutile needles in new-formed biotite. Replacement starts from the rim inward and is rarely complete. (**g**) Newly formed garnet micro-grains extending from a fragment of peak metamorphic garnet (sample EO12). The garnets form a network enclosing undeformed quartz and overgrowing S_3 muscovite. (**h**) Idiomorphic pseudomorph after staurolite, composed of sericite, chlorite and clay minerals in altered schist.

biotite is accompanied by the formation of ilmenite at the edges of the replacing muscovite. This generation of muscovite (m_3) does not appear to have a preferred orientation, suggesting recrystallization under static conditions. The final muscovite generation (m_4) defines the dominant foliation (S_3), together with a new generation of ilmenite. These muscovites are generally thin and fold around the garnet, staurolite, plagioclase and tourmaline grains, commonly with some resultant abrasion. Fracturing of these relict grains and rotation of the fragments in line with the stress direction can also be observed. The intensity of this overprint varies, with the most strongly overprinted samples preserving the earlier textures only in the pressure shadows of the relict grains. Sillimanite is converted into muscovite, while preserving its fibrolitic texture. As no overprint of S_3 muscovite on this 'fibrolitic' muscovite has been found, we infer replacement to be related to this event. Despite the textural variability in muscovite generations, there are no systematic differences in composition, indicating that recrystallization is driven by structural control. There is, however, a distinct difference in Na content between muscovites in the gneiss lenses and those in the schist matrix (Fig. 4).

Two generations of garnet can be identified in the schists. The older generation, commonly strongly resorbed at its edges, is present as large grains with aligned inclusions of ilmenite, quartz and zircon, and as euhedral inclusions in tourmaline. A decreasing spessartine content from core to rim, accompanied by a rise in the Mg number (Fig. 5), suggests that these grains formed during the prograde history, in line with their appearance as inclusions in tourmaline (see below). The rims themselves have a high spessartine content, probably related to retrograde resorption. The second and main generation of garnet consists of smaller grains, without strong resorption features, but with a

Downloaded from http://jgs.lyellcollection.org/ at Orta Dogu Teknik Universitesi on April 5, 2016

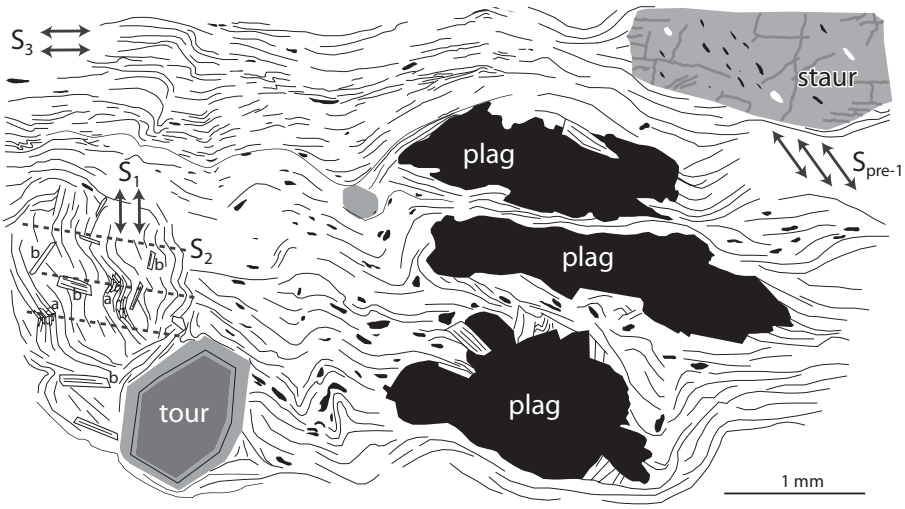


Fig. 3. Schematic drawing of schist textures and deformation sequence (compilation of textures observed in multiple samples). The peak foliation (S_1), modified by crenulation (S_2), kink bands (a, m_2) and muscovite overgrowths (b, m_3), is present as relict domains in the dominant S_3 muscovite–ilmenite foliation. The S_3 event resulted in fragmentation and abrasion of albite blasts. Inclusions in staurolite show evidence of a pre-S_1 foliation.

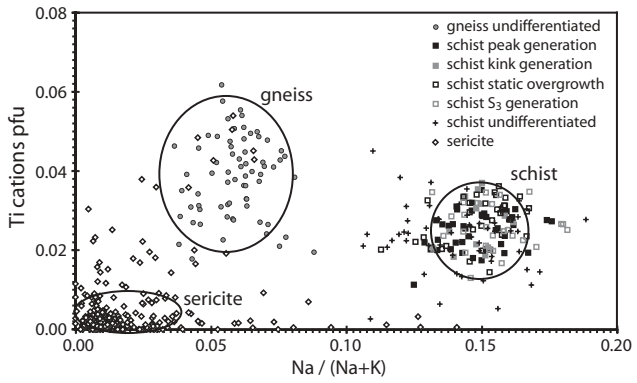


Fig. 4. Compositional variation between muscovite types in the Barlet unit. Schist muscovites are characterized by high paragonite content, whereas those from the gneisses have a higher Ti content. The muscovite generations cannot be distinguished by composition. Sericites have a limited compositional range and are characterized by low Na and Ti content.

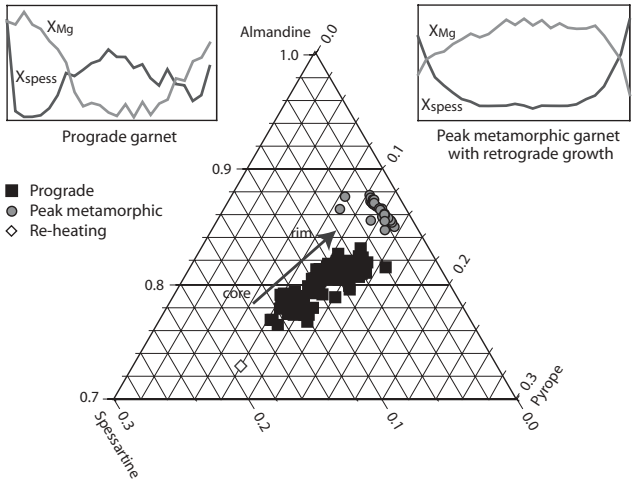


Fig. 5. Composition of garnet generations in Barlet unit schists and schematic core–rim–core profiles (insets). Prograde garnets show a distinct decrease in spessartine content from core to rim, whereas compositional variation in the cores of peak metamorphic garnets is minimal. Garnet formed during the thermal event has a high spessartine component, indicating low-temperature growth.

distinct inclusion texture. The cores of these grains are full of small pits, with a negative garnet morphology (Fig. 2b). No material was found in any of these pits. However, the texture is identical to that of garnets full of graphite inclusions in a schist we studied from Cummington, Massachusetts (unpubl. data). Where these Cummington garnets had been fractured or resorbed, the graphite was lost and pits with a similar negative crystal shape appeared. The core composition of these garnets shows little variation (Fig. 5) and no compositional zoning is present. Spessartine contents are low (X_{spes} *c.* 0.06) and the intergrowth relations between these garnets and the peak metamorphic minerals suggest that they are the peak composition. The rims do not contain any pits and show an increase in spessartine content over a wide interval. We conclude this to reflect active growth of this garnet during retrogression. The absence of any breaks in the spessartine profile appears to support this interpretation.

Plagioclase is similar to that in the gneisses. Two distinct compositions can be recognized, Ab_{99} and Ab_{90}, commonly forming alternating lamellae. We consider this to be an exsolution feature related to the peristerite solvus (Pryer & Robin 1995). The plagioclase textures reveal that they formed by blastesis, as extensive overgrowth of the peak metamorphic foliation is present. Blastesis appears to have occurred mainly in a static environment, although curvature in the foliation preserved by rotation of inclusions at the rim of a number of blasts

Downloaded from http://jgs.lyellcollection.org/ at Orta Dogu Teknik Universitesi on April 5, 2016

suggests that it is in part synkinematic. The blasts are rotated and fractured during the development of the S_3 foliation. Individual albite blasts up to 8 cm in size have been found, suggesting that the rocks may not have been a closed system at this stage. No K-feldspar has been identified in the schists.

The tourmaline grains in these samples are intensely zoned with both concentric growth zoning and hourglass sector zoning displayed. They contain inclusions of mica, quartz, ilmenite, zircon and garnet, commonly preserving an old foliation direction. The systematic disappearance of sector zoning towards the rim, together with an increasing Mg-number from core to rim, suggests an early and prograde history for the bulk of these tourmalines, although the outermost rim might record some post-peak growth (van Hinsberg *et al*. 2006).

During retrogression the remaining biotite is replaced by chlorite from the rims of the grains inward. The replacement is again accompanied by Ti exsolution, which is here stored in rutile needles in the chlorite grains, displaying a sagenitic texture (Fig. 2c and d). The intensity of the replacement varies between samples. The less-foliated parts are generally less affected by the replacement, and fresh biotite survives as inclusions in quartz and tourmaline. This patchy replacement is probably linked to the localized availability of fluids during retrogression. The retrogression event also affects garnet and staurolite, and converts both into chlorite. Staurolite is converted along cracks, whereas garnet is replaced from the rim inward. Both have a very sharp transition from replaced to fresh material. Some of the garnet shows relicts of an earlier replacement by biotite along cracks.

Temperature inversion

In several samples of Barlet unit schists, we observe that biotite, partly replaced by chlorite during retrogression, is converted back into biotite. This replacement typically starts at the rim of the chlorite grains, and is rarely complete. The exsolved rutile needles formed during initial replacement of biotite are not resorbed by the new generation of biotite (Fig. 2e and f). This allows them to be used to distinguish between biotite generations. Further, in one staurolite–garnet schist sample (EO12), a new (i.e. third) generation of garnet has been observed. This garnet is present as small grains (5–10 μm) extending from a peak garnet fragment, outlining the grain boundaries of recrystallized quartz crystals (Fig. 2g). The small garnet grains and the quartz crystals they enclose form a cluster present within the S_3 foliation. Their fragile nature suggests that they could not have survived this deformation event and must therefore postdate it. The crystals furthermore show signs of dissolution along their surfaces, suggesting that the renewed residence in the garnet stability field was a short transient stage. The composition of these small garnet grains is distinctly different from that of the earlier generations (i.e. richer in spessartine; Fig. 5).

Mineralization-related alteration

All parts of the Barlet unit, both the schist matrix and the gneiss lenses, are to some degree affected by mineralogical and textural alterations during final cooling. Its most prominent result is an intense fluid-induced sericitization, closely associated with the presence of Sb–As mineralized veins (Table 1). Alteration is most severe along vein selvages, and least intense, but still present, in samples furthest away from Sb–As veins. The feldspars, especially plagioclase, are most strongly affected by the sericitization and are commonly completely replaced by microcrystalline sericite masses. Biotite is replaced by sericite along its basal plane, whereas muscovite remains stable in the first stages of the alteration. In the final stages muscovite is also replaced by fine-grained sericite with a markedly different composition from the original muscovite (i.e. lower paragonite and Ti contents; Fig. 4). Pseudomorphs after garnet and staurolite occur as brown patches of submicroscopic intergrowths of sericite and rosette-shaped chlorites (Fig. 2h). This alteration sequence is similar to that for Sb-related hydrothermal alteration in the wider Haut-Allier area (Bril & Beaufort 1989). Chemically, the alteration amounts to metasomatism, during which all components, save those accommodated by quartz + sericite ± chlorite, are removed from the rock. Only tourmaline and apatite are unaffected.

Geothermobarometry

Prograde evolution

Ilmenite inclusions in first generation garnet provide the only quantitative data on the conditions encountered during the prograde history of the Barlet unit. Calculations using the garnet–ilmenite thermometer of Pownceby *et al*. (1991) give an average temperature of 614 °C in sample VH30 and 552 °C in sample VH04, where ilmenite is present in a more internal zone of the garnet. However, an electron probe traverse over one of these ilmenites revealed Mn diffusion from the inclusions to its host garnet, indicating that the temperatures derived are minimum estimates.

Peak metamorphism

A variety of geothermometers and barometers is available for the peak metamorphic assemblage (Table 2). Garnet–biotite thermometry has been applied using the 'average' model in the GBGASP program of Holdaway (2000), following the author's recommendations. The core composition of biotite was preferred over that of rim in actual contact with garnet, to avoid effects of late-stage re-equilibration or chloritization of the biotite rim. This composition is fairly constant for different schist samples, and is similar to that of fresh biotite inclusions in quartz, suggesting that it does indeed represent the peak composition. Similarly, the garnet composition with the lowest spessartine content in traverses over these grains was used. However, the pairs are generally less than 30 μm apart. An Fe^{3+} fraction of total iron of 0.15 was used for biotite and 0.03 for garnet as determined from microprobe analyses. Results are given in Table 2 and give an average of 658 °C at 7 kbar for 32 pairs from four schist samples.

The garnet–staurolite Fe–Mg exchange geothermometer of Fed'kin & Yakovleva (1994) has been applied to intergrowths of garnet and staurolite in samples VH30 and VH04, as well as pairs in the matrix of sample VH06. The minerals are separated by a thin (10–20 μm) band of chlorite related to retrograde replacement of staurolite. However, no compositional zoning is present in staurolite, so chlorite should not affect calculated temperatures. Results for the inclusions are 646 °C at 7 kbar and 655 °C for matrix garnet and staurolite in sample VH06 (Table 2). Attempts to use the Koch-Müller (1997) formulation give results that are unrealistic, with temperatures generally 100 °C higher. This would put these rocks well in the field of melting, no evidence for which has been found in the Barlet unit.

One of the most useful thermometers for these rocks is based on the Ti solubility in biotite. This thermometer is especially

Downloaded from http://jgs.lyellcollection.org/ at Orta Dogu Teknik Universitesi on April 5, 2016

Table 2. *Summary of thermobarometry results*

	Sample	*T* (°C)	Error	*n*	Stage
Thermometers					
Garnet–biotite (1)	VH30	662	±37	8	Peak
	VH06	659	±37	8	Peak
	VH04	655	±30	7	Peak
	EO12	656	±50	9	Peak
Garnet–staurolite (2)	VH30	654	±74	7	Peak
	VH06	655	±66	9	Peak
	VH04	636	±50	6	Peak
Garnet–ilmenite (3)	VH30	614	±69	12	Prograde
	VH04-1	549	±63	4	Prograde
	VH04-2	556	±71	4	Prograde
Garnet–muscovite (4)	VH30	610	±47	12	Retrograde
	VH04	608	±57	8	Retrograde
	EO12	599	±55	18	Retrograde
Garnet–muscovite (5)	EO12	457	±48	5	Thermal event
Ti in biotite (6)	VH30	648	±40	3	Peak
	VH06	667	±43	24	Peak
	VH04	655	±25	4	Peak
	VH60	648	±34	5	Peak
	VH15	666	±35	2	Peak
	VH17	654	±38	3	Peak
	VH58	636	±25	7	Peak
	Gneiss	665	±29	3	Peak
Ti in biotite (7)	VH30	383	±50	1	Thermal event
	VH04	355	±75	2	Thermal event
	VH06	375	±50	1	Thermal event
	EO16	374	±50	2	Thermal event
Muscovite–plagioclase (8)	VH60	612	±71	5	Retrograde
	VH30	421	±30	1	Sericitization
	VH06	293	±73	4	Sericitization
	VH60	349	±91	5	Sericitization
	VH19	309	±30	1	Sericitization
	VH17	222	±73	5	Sericitization
	VH15	212	±30	1	Sericitization
Barometers					
GRAIL (9)	VH30	7 kbar at 650 °C		10	Peak
	VH04	8 kbar at 650 °C		8	Peak
Barothermometers					
Biotite–garnet–ilmenite (10)	VH30	7.1 kbar at 629 °C		1	Peak

Summary of geothermobarometers applied and weighted average results derived for the samples. Uncertainties reported are the sum of the uncertainty reported by the authors of the formulations and the 1σ standard deviation on the average for each sample. Formulations used: 1, Holdaway (2000) GB thermometer using 'average' model at 7 kbar; 2, Fed'kin & Yakovleva (1994) assuming a pressure of 7 kbar; 3, Powneby *et al*. (1991); 4, Wu *et al*. (2002) assuming a pressure of 6 kbar; 5, Hynes & Forest (1988); 6, average of Patiño Douce (1993) and Henry *et al*. (2005) temperatures at 7 kbar; 7, Patiño Douce (1993) using α-quartz and rutile instead of β-quartz and ilmenite at 2 kbar; 8, Green & Usdansky (1986) assuming a pressure of 6 kbar for the retrograde stage and 2 kbar for sericitization; 9, Bohlen *et al*. (1983); 10, Patiño Douce *et al*. (1993).

valuable for the gneiss samples as no other ferromagnesian phases are present that might be used for geothermometry. Both the formulations of Patiño Douce (1993) and Henry *et al*. (2005) have been applied, with results overlapping and no systematic differences between the two. The biotite analyses selected are mainly from inclusions in quartz, supplemented with core analyses of fresh old biotites, similar to those used for garnet–biotite thermometry. Calculations were performed with an Fe^{3+} fraction of 0.15 for biotite, together with a hematite fraction of 0.03 for coexisting ilmenite, based on analyses of matrix ilmenites. Results for the schists give a temperature of 658 °C at 7 kbar and 665 °C for the gneisses.

Extending the Ti-in-biotite thermometer to include Mg, Fe and Al exchange on the biotite octahedral site allows simultaneous assessment of pressure and temperature from coexisting biotite, ilmenite and garnet (Patiño Douce *et al*. 1993). The thermodynamic exchange between these phases can be solved for both the Fe and Mg systems, and results should converge for a stable assemblage. Applying this thermobarometer to schist sample VH30 gives a temperature of 629 °C at a pressure of 7.2 kbar for the Mg system and 7.0 kbar for the Fe equivalent.

The albitization of plagioclase during the retrograde evolution restricts the ability to use other geobarometers, because most of these include the anorthite content of plagioclase (e.g. GASP; Holdaway 2000). However, a pressure estimate for these rocks is possible using the GRAIL barometer of Bohlen *et al*. (1983). Because the Barlet unit rocks contain ilmenite only at peak metamorphic conditions, the results give a maximum pressure estimate, which is 7 kbar for sample VH30 and 8 kbar for VH04, using a peak temperature of 650 °C.

Overall, the thermobarometers provide well-constrained peak metamorphic conditions of about 650 °C and 7 kbar for the schist matrix of the Barlet unit. Conditions for the gneisses are less well constrained. Ti-in-biotite thermometry gives a peak tem-

Downloaded from http://jgs.lyellcollection.org/ at Orta Dogu Teknik Universitesi on April 5, 2016

perature of 665 °C for these rocks, but no pressure information is available. A further indication that temperatures in the gneisses were higher than in the schists is evident from the Ti content of muscovite (i.e. a median of 0.026 c.p.f.u. in the schists and 0.039 c.p.f.u. in the gneisses, Fig. 4), because the Ti solubility in muscovite increases with temperature (Guidotti & Sassi 2002). As both rock types have ilmenite as a Ti-saturating phase, this contrast cannot be a function of bulk-rock composition.

A complementary method to assess the peak metamorphic conditions is the 'pseudo-section'approach (Holland & Powell 1998; Connolly 2005). This allows calculation of a phase-diagram section specifically for the bulk-rock composition of interest, as well as assessment of mineral compositional changes within this P–T–X space. A pseudo-section was calculated for the bulk-rock composition of schist sample VH04, using PerpleX (Connolly 2005) with the 2002 version of the Holland & Powell (1998) thermodynamic dataset. This sample does not contain albite blasts and shows minimal alteration overprint. It is thus expected to most closely resemble the peak metamorphic bulk-rock composition. Calculations were performed in the MnTiCKNFMASH system for fluid- and quartz-saturated conditions using the unconstrained minimization routine of PerpleX with the solution models Bio(HP)–Chl(HP)–Pheng(HP)–MnSt(HP)–AbPl–IlPy–Gt(HP), including all end-members of these solution models. To account for the fluid not being pure water under these conditions, an $X(CO_2)$ of 0.1 was introduced, which lowers the water activity in the fluid to less than one (CO_2 is a non-reactive component in this system). The results of this calculation (Fig. 6) constrain the assemblage in this sample to a narrow band in P–T space, and combining this with contours for the Mg-number in staurolite further refines this to conditions of about 650 °C and 7 kbar. This corresponds well to the conditions derived from geothermobarometers.

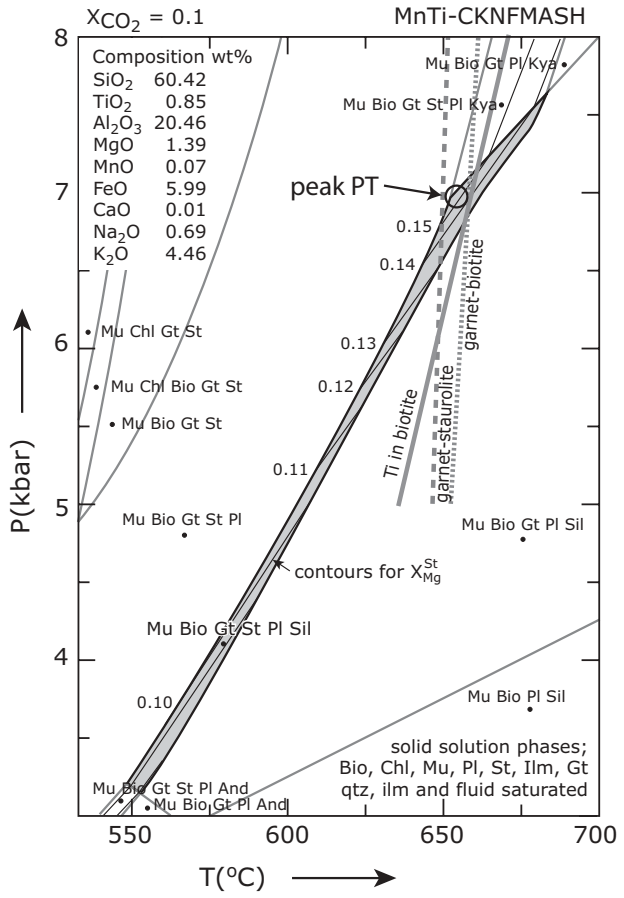


Fig. 6. Pseudo-section calculated for the bulk-rock composition of schist sample VH04, using the program PerpleX (Connolly 2005) with the 2002 update of the Holland & Powell (1998) database. Weighted average results of Ti-in-biotite, garnet–biotite and garnet–staurolite geothermometers are also shown. The peak metamorphic assemblage of garnet–staurolite–sillimanite–plagioclase–biotite–muscovite–ilmenite restricts P–T conditions to a narrow band (shaded grey). Combining this with the Mg-number of staurolite ($X_{Mg} = 0.156$) further confines conditions to a narrow region around 650 °C and 7 kbar. This agrees well with conditions derived from geothermometers as shown. Mineral solution models were used for garnet (Gt(HP)), staurolite (MnSt(HP)), plagioclase (AbPl), muscovite (Pheng(HP)), biotite (Bio(HP)), chlorite (Chl(HP)) and ilmenite (IlPy) (see www.perplex.ethz.ch for information on these solution models). Calculations were performed at quartz- and fluid-saturated conditions.

Retrograde history

A number of retrograde events can be situated in P–T space using geothermobarometers. Garnet–muscovite thermometry has been applied to pairs with peak metamorphic muscovite (m_1) and with muscovites from the dominant S_3 foliation (m_4). Temperatures from both muscovite generations are indistinguishable, resulting from the limited variation in muscovite chemistry between these generations (see Fig. 4). This probably indicates re-equilibration of all muscovites at some point in their history, and thus suggests that the temperatures derived record this re-equilibration event, rather than peak conditions. Whether the garnet also re-equilibrates during this event can be debated, but even if it does not, the muscovite in direct contact with the garnet should adjust its composition in line with the equilibrium Fe–Mg K_D at this temperature. Given the strong textural overprint of the S_3 muscovite, which was clearly accompanied by extensive muscovite new growth, we suggest that this re-equilibration event was contemporaneous with it. A temperature of 604 °C at 6 kbar was calculated for 38 pairs using the Wu *et al*. (2002) formulation (Table 2).

The peristerite gap preserved by albite grains in the schist samples provides an opportunity to set a minimum temperature boundary on the blastesis event. Analyses of albite in sample VH60 and VH06 define a minimum gap of $An_{0.4}$–$An_{10.1}$ and $An_{0.5}$–$An_{12.1}$, respectively, corresponding to temperatures of *c*. 560 and 550 °C at 5–6 kbar (Pryer & Robin 1995). Further information on the blastesis event can be gained from plagioclase–muscovite thermometry (Green & Usdansky 1986) on muscovite inclusions in albite blasts. This formulation has been applied to a section of an albite blast in schist sample VH60, which did not show any evidence of exsolution, and resulted in a temperature of 612 °C at 6 kbar. Given that blastesis texturally predates development of the S_3 foliation, this temperature fits with that derived for muscovite–garnet thermometry.

Development of a second biotite generation during reheating allows assessment of its conditions from the Ti-in-biotite thermometer of Patiño Douce (1993), after rewriting it to use α-quartz and rutile instead of β-quartz and ilmenite. The Henry *et al*. (2005) formulation cannot be used, because graphite is no longer stable. The Patiño Douce (1993) formulation is used here beyond its calibration range and the results will therefore be only semi-quantitative. Application of the thermometer is further hindered by the presence of small rutile needles in the biotite. None the

Downloaded from http://jgs.lyellcollection.org/ at Orta Dogu Teknik Universitesi on April 5, 2016

less, four samples give a consistent temperature of *c*. 375 °C at 2 kbar (Table 2) with a pressure dependence of 10 °C kbar^{-1}. A micro-garnet grown during reheating on the grain boundary of an S_3 muscovite gives a temperature of 456 °C using the garnet–muscovite thermometer of Hynes & Forest (1988) (used here because conditions are beyond the calibrated range of the Wu *et al*. (2002) thermometer). This agrees well with a temperature of 450 °C derived for these garnets using the garnet compositional contours of Spear (1993).

The conditions during hydrothermal alteration are known from fluid-inclusion studies on the resultant ore deposits and their gangue minerals (*T* is 300–400 °C for initial alteration and 250–300 °C for Sb-ore deposition; Bril *et al*. 1994, and references therein). Applying the plagioclase–muscovite thermometer of Green & Usdansky (1986) to pairs of plagioclase and the sericite replacing it gives a continuous range from about 420 °C at 2 kbar to 200 °C.

Langeac basin

Information on the thermal conditions attained in the Langeac basin can be determined from the coal grade and diagenetic mineral assemblage. Vitrinite reflectance of coal samples allows the maximum temperatures attained during coalification to be determined if the burial time is known. Folding of vitrinite reflectance patterns along with the sediments indicates that coalification predates basin inversion. This inversion is thought to have occurred at the Stephanian–Permian boundary in similar coal-bearing basins throughout the Massif Central (Robert *et al*. 1988; Courel & Liu 1991; Golitsyn *et al*. 1997). The absence of any Permian volcaniclastic deposits, so distinct in the Brassac basin to the north, agrees with basin inversion predating the Permian. On this basis, coalification took place in less than 15 Ma, which gives a maximum coalification temperature of 180 °C (Taylor *et al*. 1998). This temperature agrees well with the appearance of pyrophyllite in the deepest layers of the basin as reported by Amiot (1881), which Bouška (1981) put at *c*. 200 °C.

In a normal geothermal gradient, temperatures of 200 °C are not expected until burial depths of over 5 km (Bouška 1981). However, the present basin stratigraphy is not in accordance with such a thick sediment cover, and, throughout the Massif Central, Stephanian sequences are generally less than 1.5 km in thickness (Robert *et al*. 1988; Courel & Liu 1991; Golitsyn *et al*. 1997). Sedimentation and erosion calculations performed on other basins (e.g. the Messeix–Singles basin; Robert *et al*. 1988), indicate that a palaeocover much thicker than the present-day stratigraphy is unlikely. Simple burial is thus not sufficient to explain the high coal grade, and we therefore infer that the basin has also experienced a thermal event. The lack of evidence for a thermal event in the surrounding metamorphic units, together with the positioning of the Barlet unit and the Langeac basin next to each other, leads us to conclude that both record the same thermal event.

Synthesis

Combined petrography and geothermobarometry allow a detailed reconstruction of the Barlet area's history, which is shown schematically in Figure 7 and Table 1. The main episode of deformation and metamorphism in this part of the Variscan belt took place between 400 and 350 Ma (Ledru *et al*. 1994) and is related to the final stages of collision. The peak metamorphic conditions determined for the Barlet unit rocks are *c*. 650 °C and 7 kbar, which places them in the same realm as the Lower Allochthon schists (Santallier *et al*. 1994). Peak metamorphism is accompanied by the development of the S_1 foliation. Dating of this foliation in other parts of the Haut-Allier puts this event at 360–350 Ma (Ledru *et al*. 1994). Evidence for an earlier foliation is also present as aligned inclusions in the prograde cores of tourmaline and garnet, with an associated minimum temperature estimate of *c*. 600 °C.

Peak metamorphism is followed by development of albite blasts, which overgrow the earlier minerals and textures. Blastesis initially takes place under static conditions, but rotation of inclusions at the rim indicates the onset of renewed deformation. The static event is also preserved by a generation of muscovite (m_3), which lacks a preferred orientation. Temperature conditions for this blastesis event are *c*. 610 °C. The large size of the albite blasts suggests open-system behaviour at this time, with intro-

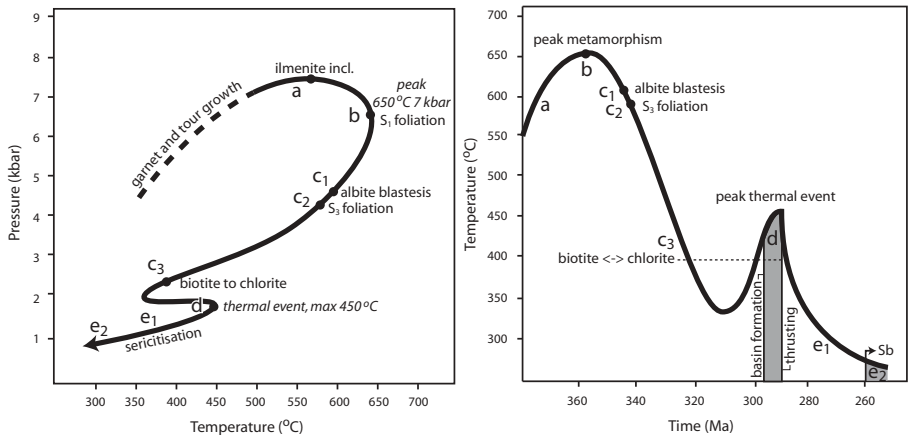


Fig. 7. Schematic *P–T* and *T–t* diagrams to summarize the evolution of the Barlet unit mélange (stage labelling corresponds to that given in Table 1). Peak metamorphism occurred at *c*. 360 Ma at 650 °C and 7 kbar. It was followed by retrograde development of albite blasts, grading into formation of the main muscovite–ilmenite dominated foliation (S_3) at *c*. 600 °C, at 340 Ma. Cooling continued until crossing of the biotite-out isograd, after which it was reversed and the rocks reheated, forming a new generation of biotite and, locally, garnet. Peak temperature conditions for this thermal event are *c.* 450 °C, and are inferred to have occurred in the Stephanian. The reheating peak is followed by intense, fluid-induced sericitization, starting at about 400 °C and continuing to the temperatures estimated for Sb-ore deposition in the Permian.

Downloaded from http://jgs.lyellcollection.org/ at Orta Dogu Teknik Universitesi on April 5, 2016

duction of Na. However, the nature of this open system, or whether it persisted, is unknown.

After appearance of albite blasts the rocks are subjected to renewed deformation, resulting in formation of the dominant muscovite–ilmenite foliation (S_3, dated at *c*. 340 Ma; Ledru *et al*. 1994). Biotite, garnet, staurolite and plagioclase grains are fragmented, abraded and rotated. Garnet–muscovite thermometry puts development of the foliation at about 600 °C, similar to albite blastesis. This suggests that the synkinematic texture preserved in the rims of albite blasts records the onset of this deformation event. Because the gneisses display only a peak metamorphic foliation (S_1, aligned with the long axis of the lenses), this indicates that they acted as rigid bodies during development of S_3, with the S_3 foliation in the schist wrapping around the lenses. This suggests that the deformation event responsible for development of S_3 is also responsible for the mélange texture of gneisses and schists in the Barlet unit.

Development of S_3 is followed by a general retrograde breakdown of the ferromagnesian phases to chlorite. The absence of deformation in the chlorite rims and lack of a preferred orientation in individual chlorite grains indicates that replacement took place after deformation ceased. Replacement of biotite is accompanied by the formation of distinct sagenitic rutile needles in the replacing chlorite.

The general retrograde cooling trend is reversed at some point after crossing the biotite to chlorite isograd. The resultant reheating causes widespread appearance of a new biotite generation in the schists, recording a reheating temperature of *c*. 380 °C. Renewed growth of garnet indicates that, at least locally, temperatures up to 450 °C were attained. Dissolution of these micro-garnets shows that renewed residence in the garnet field was short-lived. The presence of garnet in only one sample further suggests that the intensity of reheating varied on a local scale, although bulk compositional or kinetic factors cannot be ruled out. This thermal event can also be recognized in the Langeac basin sediments, where it results in anomalously high coal grades, with temperatures up to 200 °C attained at only about 1 km depth.

Based on the widespread occurrence and varied nature of thermal events in the Massif Central (e.g. Scaillet *et al*. 1996; Bouchot *et al*. 1997; Golitsyn *et al*. 1997; Marignac & Cuney 1999), we infer reheating to be regional in scale, and to have taken place in the Stephanian. This is after cooling and exhumation of the Margeride Granite (e.g. strike-slip faults related to basin formation and inversion crosscut and offset the granite). However, if heating to 450 °C was of regional extent, evidence of its effect would be expected in the other metamorphic units and in the Margeride Granite, especially as these units contain rocks with identical mineralogy, composition and texture to those found in the Barlet unit, as well as rocks more susceptible to change. Similarly, a temperature of 200 °C at a maximum burial depth of *c*. 1 km in the Langeac basin is difficult to accommodate by regional heating. We therefore propose local concentration and upward transfer of this regional heat by fluids, along the crustal-scale faults that were (re-)activated in the Neo-Variscan (e.g. the Grand Silon Houiller as well as the faults responsible for the Langeac basin). This fluid-induced heating is similar to the model proposed by Golitsyn *et al*. (1997) for coalification in the Blanzy–Montceau basin, but we extend it here to facilitate silicate reactions at higher temperatures.

Basin inversion follows the thermal event's peak and results in thrusting of the Langeac basin onto the metamorphic basement. The Barlet unit is also thrust in a SE direction at this stage, locally over the Leptyno-Amphibolite Complex and onto the Lower Allochthon schists. The absence of thrusting in the other basement units, and the similarity in shape between the Barlet unit and the Langeac basin, suggests that thrusting of the Barlet unit was a direct result of the presence of the basin.

Final cooling appears to be continuous, in both conditions and textures (e.g. sulphide–sericite pseudomorphs after feldspar), with the development of hydrothermal Sb–As mineralization in the Barlet unit rocks. Sericitization commences at around 400 °C and continues to temperatures determined for the Sb deposits (250–300 °C; Bril *et al*. 1994). This suggests a genetic link between the thermal event and the subsequent hydrothermal episode, and we propose that the fluid causing reheating of the metamorphic basement in the Stephanian was in fact responsible for the formation of Sb–As mineralization in the Permian.

Overall, this work brings together in one area the various lines of evidence for a Massif Central regional-scale thermal event and shows how the different expressions of this event are connected, from regional retardation of granite cooling to localized reheating of the basement and anomalous coalification as a result of upward transfer of heat by fluids, and to ore deposition by these fluids during final cooling.

We are grateful to M. Cuney, Henri Poincaré University, Nancy, for discussions on the metallogeny and geological history of the French Variscides. We are also greatly indebted to A. Andrieu for preserving, and making available to us, the old mining reports of the Langeac basin coal mines. We also thank A. Kronz, University of Göttingen, for his help with electron microprobe analyses, S. Verdegaal and L. van Doorn for coal analyses, and D. Robinson for comments on an earlier draft of this manuscript. We thank P. Goncalves and an anonymous reviewer for their insightful comments, which improved the clarity of the manuscript.

References

Amiot, M. 1881. Bassin houiller de Langeac. *Études des Gites minéraux de la France*. A. Quantin, Paris, 288–317.

Bohlen, S.R., Wall, V.J. & Boettcher, A.L. 1983. Experimental investigations and geological applications of equilibria in the system $FeO–TiO_2–Al_2O_3–SiO_2–H_2O$. *American Mineralogist*, **68**, 1049–1058.

Bouchot, V., Milesi, J.P., Lescuyer, J.L. & Ledru, P. 1997. Les minéralisations aurifères de la France dans leur cadre géologique autour de 300 Ma. *Chronique de la Recherche Minière*, **528**, 13–62.

Bouška, V. 1981. Coalification. *In:* Bouška, V. (ed.) *Geochemistry of Coal*. Elsevier, Amsterdam, 96–127.

Bril, H. 1983. *Etude métallogénique des minéralisations à antimoine et associées du district de Brioude–Massiac (Massif Central français), conditions de dépot; implications genetiques*. Thèse de doctorat d'Etat, Université de Clermont-Ferrand II.

Bril, H. & Beaufort, D. 1989. Hydrothermal alteration and fluid circulation related to W, Au and Sb vein mineralisations, Haut Allier, Massif Central, France. *Economic Geology*, **84**, 2237–2251.

Bril, H., Marignac, C., Cathelineau, M., Tollon, F., Cuney, M. & Boiron, M.C. 1994. Metallogenesis of the French Massif Central: time–space relationships between ore deposition and tectono-magmatic events. *In:* Keppie, J.D. (ed.) *Pre-Mesozoic Geology in France and Related Areas*. Springer, Berlin, 379–402.

Burg, J.P., Leyreloup, A., Marchand, J. & Matte, Ph. 1984. Inverted metamorphic zonation and large-scale thrusting in the Variscan belt: an example in the French Massif Central. *In:* Hutton, D.H.W. & Sanderson, D.J. (eds) *Variscan Tectonics of the North Atlantic Region*. Geological Society, London, Special Publications, **14**, 47–61.

Connolly, J.A.D. 2005. Computation of phase equilibria by linear programming: a tool for geodynamic modeling and its application to subduction zone decarbonation. *Earth and Planetary Science Letters*, **236**, 524–541.

Copard, Y., Disnar, J.R., Becq-Giraudon, J.-F. & Boussafir, M. 2000. Evidence and effects of fluid circulation on organic matter in intramontane coalfields (Massif Central, France). *International Journal of Coal Geology*, **44**, 49–68.

Courel, L. & Liu, X.B. 1991. Variations in the geothermal history in coal basins; relationship with basin dynamics. *Bulletin de la Société Géologique de France*, **162**, 363–370.

Couturié, J.P. & Vachette, M. 1980. Age Westphalien des leucogranites

Downloaded from http://jgs.lyellcollection.org/ at Orta Dogu Teknik Universitesi on April 5, 2016

recoupant le granite de la Margeride. *Comptes Rendus de l'Académie des Sciences, Série IIA*, **291**, 43–45.

Couturié, J.P., Vachette, M. & Vialette, Y. 1979. Age Namurien d'un laccolite granitique différencié par gravité: le granite de la Margeride (Massif Central français). *Comptes Rendus de l'Académie des Sciences, Série IIA*, **289**, 449–452.

Derré, C. 1972. *Histoire des filons de fluorine et du bassin houiller de Langeac*. Thèse 3ème cycle, Université de Paris VI.

Faure, M. 1995. Late orogenic Carboniferous extensions in the Variscan French Massif Central. *Tectonics*, **14**, 132–153.

Faure, M., Monie, P., Pin, C., Maluski, H. & Leloix, C. 2002. Late Viséan thermal event in the northern part of the French Massif Central: new $^{40}Ar/^{39}Ar$ and Rb–Sr isotopic constraints on the Hercynian syn-orogenic extension. *International Journal of Earth Sciences*, **91**, 53–75.

Fed'kin, V.V. & Yakovleva, L. 1994. Experimental study of staurolite–garnet exchange equilibrium. *Dokladi Akademii Nauk SSSR*, **339**, 234–238.

Forestier, F.H. 1961. *Métamorphisme hercynien et anté-hercynien dans le basin du Haut-Allier (Massif Central français)*. Thèse d'Etat, Université de Clermont-Ferrand.

Golitsyn, A., Courel, L. & Debriette, P. 1997. A fault-related coalification anomaly in the Blanzy–Montceau Coal Basin (Massif Central, France). *International Journal of Coal Geology*, **33**, 209–228.

Green, N.L. & Usdansky, S.I. 1986. Toward a practical plagioclase–muscovite geothermometer. *American Mineralogist*, **71**, 1109–1117.

Guidotti, C.V. & Sassi, F.P. 2002. Constraints on studies of metamorphic K–Na white micas. *In:* Mottana, A., Sassi, F.P., Thompson, J.B. & Guggenheim, S. (eds) *Micas: Crystal Chemistry and Metamorphic Petrology.* Mineralogical Society of America, Reviews in Mineralogy and Geochemistry, **46**, 413–448.

Henry, D.J., Guidotti, C.V. & Thomson, J.A. 2005. The Ti-saturation surface for low-to-medium pressure metapelitic biotite: implications for geothermometry and Ti-substitution mechanisms. *American Mineralogist*, **90**, 316–328.

Holdaway, M.J. 2000. Application of new experimental and garnet Margules data to the garnet–biotite geothermometer. *American Mineralogist*, **85**, 881–892.

Holland, T.J.B. & Powell, R. 1998. An internally consistent thermodynamic data set for phases of petrological interest. *Journal of Metamorphic Geology*, **16**, 309–343.

Hynes, A. & Forest, R.C. 1988. Empirical garnet–muscovite geothermometry in low-grade metapelites, Selwyn Range (Canadian Rockies). *Journal of Metamorphic Geology*, **6**, 297–309.

Koch-Müller, M. 1997. Experimentally determined Fe–Mg exchange between synthetic staurolite and garnet in the system $MgO–FeO–Al_2O_3–SiO_2–H_2O$. *Lithos*, **41**, 185–212.

Lafon, J.M. & Respaut, J.P. 1988. Uranium–lead geochronology and Variscan leucogranites. Examples from the Grandrieu and La Porcherie leucogranites (French Massif Central). *Bulletin of Mineralogy*, **111**, 225–237.

Ledru, P., Lardeaux, J.M. & Santallier, D. *et al.* 1989. Où sont les nappes dans la Massif Central français? *Bulletin de la Societé Géologique de France*, **8**, 605–618.

Ledru, P., Costa, S. & Echtler, H. 1994. Structure. *In:* Keppie, J.D. (ed.) *Pre-Mesozoic Geology in France and Related Areas*. Springer, Berlin, 305–323.

Ledru, P., Courrioux, G., Dallain, C., Lardeaux, J.M., Montel, J.M., Vanderhaeghe, O. & Vitel, G. 2001. The Velay dome (French Massif Central): melt generation and granite emplacement during orogenic evolution. *Tectonophysics*, **342**, 207–237.

Malavieille, J., Guihot, P., Costa, S., Lardeaux, J.M. & Gardien, V. 1990. Collapse of the thickened Variscan crust in the French Massif Central: Mont Pilat extensional shear zone and St. Etienne Late Carboniferous basin. *Tectonophysics*, **177**, 139–149.

Marchand, J., Bouiller, R., Burg, J.P., Cornen, G., d'Arcy, D., Becq-Giraudon, J.F. & Vautrelle, C. 1989. *Notice explicative, Carte géologique de la France (1/50 000), feuille Langeac (790)*. BRGM, Orleans.

Marignac, C. & Cuney, M. 1999. Ore deposits of the French Massif Central: insight into the metallogenesis of the Variscan collision belt. *Mineralium Deposita*, **34**, 472–504.

Matte, Ph. 1991. Accretionary history and crustal evolution of the Variscan belt in Western Europe. *Tectonophysics*, **196**, 309–337.

Ménard, G. & Molnar, P. 1988. Collapse of a Hercynian Tibetan plateau into a late Palaeozoic European Basin and Range province. *Nature*, **334**, 235–237.

Patiño Douce, A.E. 1993. Titanium substitution in biotite: an empirical model with applications to thermometry, O_2 and H_2O barometries, and consequences for biotite stability. *Chemical Geology*, **108**, 133–162.

Patiño Douce, A.E., Johnston, A.D. & Rice, J.M. 1993. Octahedral excess mixing properties in biotite: a working model with applications to geobarometry and geothermometry. *American Mineralogist*, **78**, 113–131.

Périchaud, J.J. 1980. L'antimoine, ses minerais et ses gisements. Synthèse gitologique sur les gisements du Massif Central français. *Chronique de la Recherche Minière*, **456**, 5–64.

Ploquin, A. & Stussi, J.M. 1994. Felsic plutonism and volcanism in the Massif Central. *In:* Keppie, J.D. (ed.) *Pre-Mesozoic Geology in France and Related Areas*. Springer, Berlin, 363–378.

Powneby, M.I., Wall, V.J. & O'Neill, H.S.C. 1991. An experimental study of the effect of Ca upon garnet–ilmenite Fe–Mn exchange equilibria. *American Mineralogist*, **76**, 1580–1588.

Pryer, L.L. & Robin, P.Y.F. 1995. Retrograde metamorphic reactions in deforming granites and the origin of flame perthite. *Journal of Metamorphic Geology*, **13**, 645–658.

Respaut, J.P. 1984. *Géochronologie et géochimie isotopique U–Pb de la minéralisation uranifère des Pierres Plantées (Lozère) et de son encaissant: le massif granitique de la Margeride*. Thèse 3ème cycle, Université de Montpellier.

Robert, P. 1989. The thermal setting of Carboniferous basins in relation to the Variscan orogeny in Central and Western Europe. *International Journal of Coal Geology*, **13**, 171–206.

Robert, P., Berquer, C., Courel, L., Kubler, B. & Robert, P. 1988. Anomalie thermique précoce dans le bassin houiller stéphanien de Messeix-Singles, Massif Central français. *Sciences Géologique Bulletin, Strasbourg*, **41**, 333–349.

Santallier, D.S., Lardeaux, J.M., Marchand, J. & Marignac, C. 1994. Metamorphism. *In:* Keppie, J.D. (ed.) *Pre-Mesozoic Geology in France and Related Areas*. Springer, Berlin, 324–340.

Scaillet, S., Cuney, M., le Carlier de Veslud, C., Cheilletz, A. & Royer, J.J. 1996. Cooling pattern and mineralization history of the Saint Sylvestre and western Marche leucogranite pluton, French Massif Central: II. Thermal modelling and implications for the mechanisms of uranium mineralization. *Geochimica et Cosmochimica Acta*, **60**, 4673–4688.

Spear, F.S. (ed.) 1993. *Metamorphic Phase Equilibria and Pressure–Temperature–Time Paths*. Mineralogical Society of America, Monographs, **1**.

Taylor, G.H., Teichmüller, M., Davies, A., Diessel, C.F.K., Littke, R. & Robert, P. 1998. *Organic Petrology.* Bornträger, Berlin.

van Hinsberg, V.J., Schumacher, J.C., Kearns, S., Mason, P.R.D. & Franz, G. 2006. Hourglass sector zoning in metamorphic tourmaline and resultant major and trace element fractionation. *American Mineralogist*, **91**, 717–728.

van Hinsberg, V.J., Zinngrebe, E., de Wijs, C.J. & Vriend, S.P. 2003. A new model for Sb deposition in the French Massif Central based upon thermodynamic modeling of the mineralizing fluid. *Journal of Exploration Geochemistry*, **78-79**, 75–79.

Wu, C.M., Wang, X.S., Yang, C.H., Geng, Y.S. & Liu, F.L. 2002. Empirical garnet–muscovite geothermometry in metapelites. *Lithos*, **62**, 1–13.

Received 13 December 2005; revised typescript accepted 9 August 2006.
Scientific editing by Mike Fowler